IEEE Access
Multidisciplinary | Rapid Review | Open Access Journal

Received 24 September 2022, accepted 14 October 2022, date of publication 19 October 2022, date of current version 26 October 2022.

Digital Object Identifier 10.1109/ACCESS.2022.3215468

RESEARCH ARTICLE

A Cutter Selection Method for 2 1/2-Axis Trochoidal Milling of the Pocket Based on Optimal Skeleton

FEIYAN HAN, LONGLONG HE, ZHITAO HU, AND CHUANWEI ZHANG
School of Mechanical Engineering, Xi'an University of Science and Technology, Xi'an 710000, China

Corresponding author: Feiyan Han (hanfeiyan@126.com)

This work was supported in part by the National Natural Science Foundation of China under Grant 51905418, in part by the Coal Joint Fund Project of Shaanxi under Grant 2019JLM-37, in part by the Excellent Youth Fund of the Xi'an University of Science and Technology under Grant 2020YQ3-07, and in part by the Opening Topic Fund of Key Laboratory of Aeroengine High Performance Manufacturing Industry and Information Technology of Ministry of China under Grant HPM-2020-04.

ABSTRACT The trochoidal toolpath is generated based on skeleton. However, several different skeletons can be extracted from one pocket. To improve the efficiency of trochoidal rough milling, a cutter selection method basing the optimal skeleton is proposed. Firstly, for a pocket, preliminary skeleton curves and nodes are extracted according to the principle of medial axis transformation. A skeleton extraction method is given that the skeleton is a combination of skeleton curves generated by randomly connecting the preliminary skeleton curves under nodes constraint. A set of skeletons can be obtained by repeatedly extracting skeleton. Furthermore, an optimization model based on the shortest machining time is established, and then the optimization model is solved by the Genetic Algorithm to determine the optimal tool combination and skeleton. The developed approach is validated in trochoidal milling a pocket for cutter selection. The experimental results show that the method can significantly improve the processing efficiency.

INDEX TERMS Cutting tools, genetic algorithm, milling, skeleton.

I. INTRODUCTION

Trochoidal milling, which can mill away large volume of material from the workpiece, is widely used in computer numerical control (CNC) milling [1]. Machining time saving can be achieved by selecting proper cutters. However, the selection of tools mainly comes from machining practice, which is time-consuming and largely depends on the engineers' experience [2], [3].

The selection of cutters for 2 1/2 -Axis trochoidal milling has been addressed by several researchers. Xiong et al. [4] proposed a region division method based on Voronoi diagram, which can divide processing region into large circular and elongated regions, and then two regions are processed by different tools and tool paths. Ferreira and Ochoa [5] presented a simple method of trochoidal tool selection based on medial axis transformation. In this method, several feasible tool combinations are selected from a given toolset according to the medial axis transformation, and then the optimal tool combination is selected by comparing the processing time of trochoidal milling using these tool combinations. This method is further verified in practical processing [6]. Although the tool selection methods in trochoidal milling are few, the problem of tool selection in traditional milling has been addressed by lots of researchers. The selection of tool size mainly uses geometric information to calculate tool diameter. The optimization method of dividing machining area based on the Voronoi diagram or distance field to obtain a toolset has been widely used [7], [8], [9], [10]. Phung et al. [11] established an automatic tool selection model based on machining feature characteristics, and utilized the decision method with integrated fuzzy analytic hierarchy process to solve this model to determine the tool sequence. Ba et al. [12] proposed a multi-tool selection method based on the

The associate editor coordinating the review of this manuscript and approving it for publication was Le Hoang Son.

medial axis transformation. Li et al. [13] established the tool optimization model based on the characteristic point on the medial of the machining area, and solved it through the particle swarm optimization algorithm. Shi et al. [14] systematically analyzed the influence of tool selection on energy efficiency in the milling process. It was found that the rank of influence is cutter radius > flute number > helix angle. In order to reduce the energy consumption of the machine tools, Li et al. [15] presented an optimization method of tool combination selection based on the integration of directed graph and Dijkstra algorithm. Zhao et al. [16] introduced STEP-NC standard as the constraint condition for tool selection model based on minimum energy consumption. Wang et al. [17] proposed a tool selection method based on Genetic Algorithm and image skeleton. Wang's method takes the maximum material removal rate of the workpiece as the optimization target and optimizes the tool combination through the GA. Jayanthi [18] proposed an optimization model for tool selection based on the shortest machining time, and then the optimal tools can be determined by using the optimization algorithm to solve this model (Two optimization algorithms are explained here: Dijkstra and Genetic Algorithm). Results show that using the GA can save computation time but generate inexact optimal solution compared to using the Dijkstra algorithm. In recent years, deep learning has been widely used in machining automation, and has improved machining quality and efficiency to a certain extent [19], [20]. Checa et al. [21] applied the machine learning technology to analyze the experimental data in milling with different geometric parameters, and then established the tool selection model to acquire suitable tools in a short computer time. In summary, it can be seen from the above-mentioned literatures that the automatic tool selection method with advanced algorithms has been widely studied in traditional milling but not in trochoidal milling. Therefore, automatic tool selection in trochoidal milling needs to be developed.

Extracting the skeleton from the pocket is a necessary step in trochoidal milling because the trochoidal path is generated based on the skeleton. Che et al. [22] proposed a skeleton extraction method. In this method, the initial skeleton is firstly obtained by Euclidean distance field transformation on the surface of the workpiece, and then the initial skeleton is guided to the correct position by utilizing the snake model. Ferreira et al. [5] extracted the skeleton of the pocket based on the medial axis transformation, and then applied this skeleton to generate the trochoidal path. The skeleton, which is the basis for generating trochoidal path, is a collection of skeleton curves, but some of these curves could intersect. Multiple different trochoidal tool paths can be generated because of these intersections (see Fig. 1). Different trochoidal tool path will result in different processing time.

Therefore, the influence of skeleton on the generation of trochoidal toolpath should be considered in the selection of trochoidal tools. Nevertheless, few studies focus on the influence of skeleton on tool optimization of trochoidal milling.

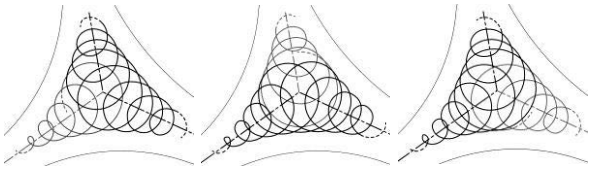

FIGURE 1. The trochoidal path is generated in the case of intersecting skeleton curves.

Intersecting skeleton curves in a skeleton result in multiple different trochoidal tool path, which is a challenge to select trochoidal cutters scientifically. Change your mind, it is assumed that the generation of trochoidal toolpath depends on the skeleton curves in the skeleton, and has nothing to do with whether the skeleton curves intersect. If a set of skeletons whose skeleton curves do not intersect could be extracted from a pocket, the total processing time can be calculated for milling this pocket using the tool combination and skeleton, which are selected from the given toolset and skeleton set, respectively. The optimal tool combination and skeleton can be obtained by comparing these total machining times.

Therefore, an automatic selection method of trochoidal cutter based on optimal skeleton is proposed. The rest of this paper is organized as follows: In Section 2, the method of skeleton extraction is presented, which provides convenience for the establishment of tool optimization model. In Section 3, an optimization model is established and solved by GA to acquire the optimal tool combination and skeleton. The simulation results are shown in Section 4. The conclusions of this paper are given in Section 5.

II. SKELETON EXTRACTION

Skeleton extraction is foundational for trochoidal milling. A method to extract skeleton for pocket is proposed, and the details are introduced in this section.

A. FEATURE POINTS EXTRACTION

The feature points of the skeleton must be obtained before the skeleton of the pocket is extracted. In this section, the feature points will be extracted according to the principle of medial axis transformation.

According to the processing accuracy, the processing area of the pocket is transformed into a pixel image (See Fig. 2). There are three types of pixels in the pixel image, which represent the interior ∂I, boundary ∂B, and exterior ∂E of the processing area.

The calculation of distance field is widely used in computer graphics processing. For two pixels $P(x_1, y_1)$ and $Q(x_2, y_2)$, the Euclidean distance d is defined as $d(P, Q) = \sqrt{(x_1 - x_2)^2 + (y_1 - y_2)^2}$, where x and y refer to the row and column numbers of pixel. The Euclidean distance field of the

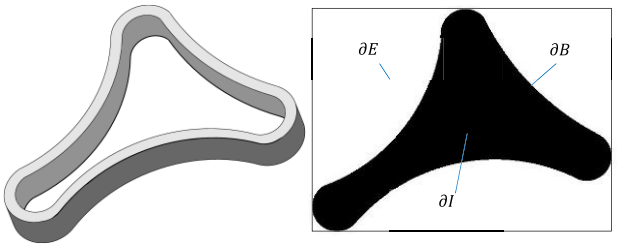

(a) Part 1 (b) Transformed pixel image

FIGURE 2. The processing area of the Part I is transformed into a pixel image.

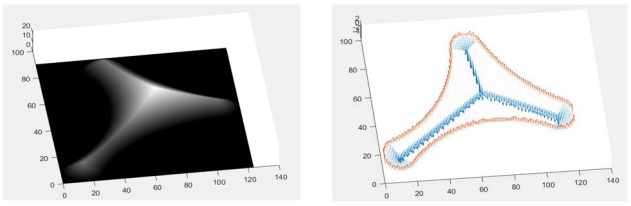

(a) The three-dimensional grayscale (b) Laplacian value plotted as vector over the XY plane of the grayscale image

FIGURE 3. Grayscale image and its Laplacian processing result.

pixel image can be expressed as:

$$LIC\,(P) = \begin{cases} \min\limits_{Q\in\partial B}(d(P,Q)) & P \in (\partial I \cup \partial B) \\ 0 & P \in \partial E \end{cases} \tag{1}$$

$LIC\,(P)$ represents the maximum allowable radius of the cutting tool centered on point $P\,(x_1, y_1)$, when milling a pocket without excessive material removal. That is, the tool radius should be less than $LIC\,(P)$ when the tool center position is point P.The Euclidean distance field of the pixel image is displayed as the three-dimensional grayscale image shown in Fig. 3(a), where the value of the Z-axis is equal to the LIC value of the corresponding pixel point.

The Laplacian discrete operator is commonly used in edge detection for image processing. It provides a facile method to acquire the concavity/convexity of the surface. This operator is implemented on the grayscale image by setting a matrix convolution ∇ as kernel. The matrix is expressed as:

$$\nabla = \begin{bmatrix} 1 & 1 & 1 \\ 1 & -8 & 1 \\ 1 & 1 & 1 \end{bmatrix} \tag{2}$$

After processing the grayscale image with Laplace transform, the result is shown in Fig. 3 (b), where the direction and length of the vector represent the plus-minus and the size of the Laplacian values, respectively. (The upward vector displayed in red represents the positive Laplace value, while the downward vector displayed in blue represents the negative Laplacian value.)

It can be seen from Fig. 4 (b) that pixels with negative Laplacian values are close to the skeleton of the processing area, but some of them do not belong to the skeleton. Therefore, the Pixel with negative Laplacian value that is not part of the skeleton should be filtered. This problem is further solved by vector image, which indicates the direction from the pixel (∂I) to the nearest boundary. The pixel P_0 is not regard as a skeleton point if all the vector angle between adjacent pixels of pixel P_0 are less than a constant δ, ($\delta = 15^o$). The detail of the vector image is shown in Fig. 4(a). The final feature points are shown in Fig. 4(c).

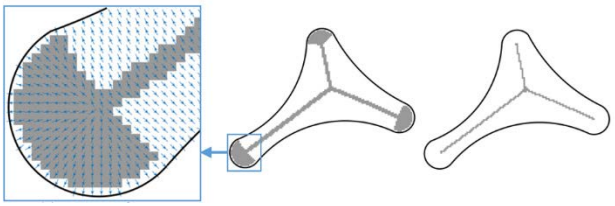

(a) Vector image (b) Points with negative Laplacian (c) Feature points after filtering

FIGURE 4. The filtering processes of feature points.

B. EXTRACTION OF SKELETON AND SKELETON SET

In order to extract the skeleton of the pocket, the preliminary skeleton curves and nodes are firstly acquired according to the feature points, and then the skeleton of the pocket can be obtained by establishing the relationship between the primary skeleton curves and the skeleton. The skeleton set can be finally obtained by repeatedly extracting the skeleton.

1) EXTRACTION OF THE PRELIMINARY SKELETON CURVES

Step 1: The feature points are fitted to generate a preliminary skeleton curve l_k until the tangent vector of the curve suddenly changes. Then this curve l_k is added into the preliminary skeleton set L.

Step 2: Repeat Step 1 until all feature points have been fitted.

The preliminary skeleton curve set L can be expressed as:

$$L = \{l_k | k = 1, 2, \cdots, n\} \tag{3}$$

where l_k represents the k^{th} curve in the preliminary skeleton curve set. If three or more endpoints of the preliminary curve coincide in the same position, this position is defined as a node. The corresponding node information can be obtained after the preliminary skeleton curves set was extracted.

2) EXTRACTION OF THE SKELETON

Step 1: Randomly select a curve l_i from the preliminary skeleton curve set L and delete this curve in the set L.

Step 2: If any curves in set L share the same node as curve l_i, randomly select a curve (l_j) from those curves, then connect curve l_j to the curve l_i, $(l_i = l_i + l_j)$, and lastly delete curve l_j from the set L. Otherwise, the curve l_i will be recorded as the final skeleton curve $(G_{k,e})$ and added into the skeleton (G_k). and then return to Step 1.

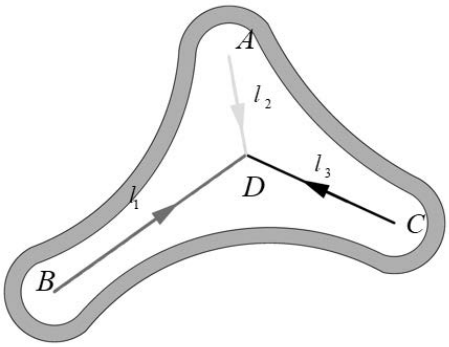

FIGURE 5. All the Preliminary skeleton curves of the Part I.

TABLE 1. The skeleton set of the part I.

Skeleton set \ Skeleton	Skeleton curve $G_{i,1}$	Skeleton curve $G_{i,2}$
G_1	$l_1 - l_2$	l_3
G_2	$l_1 - l_3$	l_2
G_3	$l_2 - l_3$	l_1

Step 3: Repeat Step 2 until the preliminary skeleton curve set L is empty.

The skeleton (G_k) can be expressed as:

$$G_k = \left\{G_{k,e} | e = 1, 2, \cdots, m\right\} \tag{4}$$

The connection relationship of skeleton curves is variable, so one or more skeletons can be extracted from one pocket.

For a complex pockets, it is impossible to obtain all the skeletons by a simple mathematical formula [23]. Therefore, this paper will utilize the computer to search skeletons which constitute the skeleton set: The skeleton set (G) is empty before the search begins. A skeleton (G_k) of the pocket can be acquired by performing Section 2.B(2) (i.e. section "EXTRACTION OF THE SKELETON"). If skeleton G_k differs from all elements of the skeleton set G, the skeleton G_k will be added into the skeleton set G.

The obtained skeleton set G will be closer to the maximum skeleton set of the pocket with the increasing of Section 2.B(2) performing times. The obtained skeleton set G can be expressed as:

$$G = \{G_k | k = 1, 2, \cdots, g\} \tag{5}$$

where G_k represents the k^{th} skeleton in skeleton set G.

The above method is applied to a pocket to obtain all the preliminary skeleton curves l_1, l_2 and l_3 (see Fig. 5). And then, as shown in Table 1, the skeleton set including three skeletons (G_1, G_2 and G_3) is obtained.

III. TOOL SELECTION OF TROCHOIDAL MILLING

The larger the diameter of the tool used for milling a workpiece, the shorter the tool path, but the more uncut material. The processing time is affected by the path and feed speed of the tool. To improve processing efficiency and ensure adequate material removal, a set of cutting tools will be given, from which a limited number of tools are selected to process the pocket. This section discusses how to select the optimal tools according to certain constraints.

A. EATABLISHMENT OF OPTIMIZATION MODEL FOR TOOL SELECTION

The trochoidal path is generated based on skeleton. Therefore, when trochoidal milling a pocket with the same tools, different skeleton will result in different machining regions, the number of tool lifting, tool paths, and even machining time. In order to enhance machining efficiency, it is necessary to establish an optimization model of trochoidal tool selection based on skeleton.

Total machining time is the best standard to measure machining efficiency. The total machining time in the milling process is formed by the time of trochoidal toolpath and the time of non-trochoidal toolpath, here, the time of non-trochoidal toolpath includes the tool change time and the transition time of the tool between different machining regions. Then, the total machining time can be expressed as:

$$T = T_{Machine} + T_{Change} + T_{Transition} \tag{6}$$

where $T_{Machine}$ represents the time of trochoidal toolpath, T_{Change} is the tool change time, $T_{Transition}$ is the transition time of the tool between different machining regions.

Given the available set of cutting tools $\Omega_o = \{D_i | i = 1, 2, \cdots, n\}$, Suppose given cutting tool number m, ($m \leq n$). Then a set of tools Ω will be selected from the set Ω_o to process the pocket.

$$\Omega \subseteq \Omega_o \tag{7}$$

where $\Omega = \{D_i | i = 1, 2, \cdots, m\}$.

Since the machining time is dependent on the tool and skeleton chosen, the total machining time can be expressed as:

$$\begin{aligned} T &= T(\Omega, G_k) = T_{Machine} + T_{Change} + T_{Transition} \\ &= \sum_{i=1}^{m} \sum_{j=0}^{h} \frac{w_{i,j}}{f_i} + \sum_{i=2}^{m} \tau_i + \sum_{i=1}^{m} \sum_{j=2}^{e} \xi_{i,j} \end{aligned} \tag{8}$$

where f_i is the feed speed of the i^{th} tool, $w_{i,j}$ is the length of the trochoidal toolpath when the i^{th} tool is used for the j^{th} machining, τ_i is the time for changing the current tool from the $(i-1)^{th}$ tool to the i^{th} tool in set Ω. $\xi_{i,j}$ is the j^{th} transition time of the i^{th} tool between different machining regions.

In 2.5-axis milling, the area of rest uncut material after processing can represent the quality of the product. A proper processing should satisfy the following relationship:

$$S = S(\Omega, G_k) = \frac{\partial - \sum_{i=1}^{m} \sum_{j=0}^{k} \partial_{i,j}}{\partial} \times 100\% \leq \varepsilon \tag{9}$$

where: $\partial_{i,j}$ is the number of pixels cut by the i^{th} tool for the j^{th} machining. ∂ is the total number of pixels to be cut, (i.e. ∂ is

the number of ∂I). After processing finished, the ratio of the rest uncut area to the area to be processed must be less than the constant ε.

B. GENERATION OF TROCHOIDAL TOOL PATH

The machining time is mainly related the total length of tool path along the surface to be machined (see Eq. (8)), and the tool path has effect on the motion characteristics of machine tool in milling. Therefore, generating the proper trochoidal tool path is beneficial to improve the machining efficiency and suitable for the movement of machine tool.

There are two toolpath models in trochoidal milling: (1) The circular path, which is usually connected by adjacent circles and straight lines [24]. (2) The trochoidal (TR) path, which has continuous tangents and curvature, is generated by a complex curve without any straight line [25], [26], [27], [28].

Although the circular path model has been widely used in machining, processing workpiece using the circular path model will lead to discontinuous acceleration of machine tool [25]. However, the speed and acceleration of machine tool are continuous when the workpiece is processed using the TR path model. That is to say, TR path model is more suitable for the motion characteristics of the machine tool than circular path model. In addition, the length of the TR path model is shorter than that of the circular path model when the step distance is the same. That is to say, the processing efficiency of the TR path model is higher than that of the circular path model [18], [19], [20], [21], [22], [23], [24], [25], [26]. By comparing those two toolpath models, this paper will adopt TR path model as the actual tool path to mill a pocket.

The trochoidal path (TR) is shown in Fig. 6, in one trochoidal period, the instantaneous centre of the tool moves linearly from O_1 to O_2, O_1 and O_2 are located on the skeleton curve with distance s (s denoted the step length), Furthermore, the instantaneous centre of the tool can be parameterized by the revolution angle θ; here, θ belongs to the range $[0, 2\pi]$. The geometric relationship of the trochoidal path can be expressed as:

$$\begin{cases} X = R_C sin\,\theta \\ Y = \dfrac{s\theta}{2\pi} - R_C cos\,\theta \end{cases} \tag{10}$$

In order to achieve continuous tangent and curvature of trochoidal path in two trochoidal periods, the revolution radius of the tool can be expressed as:

$$R_C = (LIC(O_1) - R_T)(1 - \frac{\theta}{2\pi}) + (LIC(O_2) - R_T)\frac{\theta}{2\pi} \tag{11}$$

where: $LIC(O_1)$ and $LIC(O_2)$represent the maximum radius of the cutting circle centered on points O_1 and O_2, respectively. R_T is the tool radius.

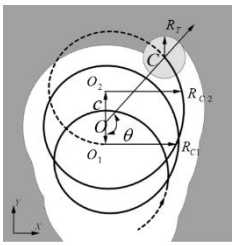

FIGURE 6. Trochoidal (TR) path.

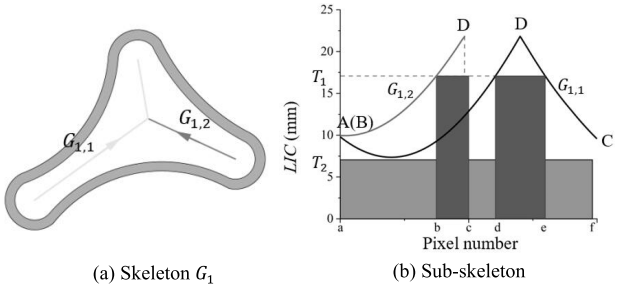

FIGURE 7. The feasible range of tool is distributed along the skeleton curve in the skeleton G_1.

C. DIVISION OF MACHINING REGION

Dividing the machining region according to different tool is an important step of multi-tool selection. This section will discuss in detail the division of machining region.

1) FEASIBLE TOOL REGION

Since the skeleton is a complete descriptor of pocket shape, skeleton curves and their *LIC* value are compact representations of pocket geometric and topological features. Therefore, the largest tool radius distribution along the skeleton curves can be determined based on the skeleton; simultaneously, a feasible machined region of each tool in the toolset can be obtained.

Part I is still used to illustrate the relationship between the skeleton and the machinable region of the tool as an example. The skeleton of this pocket is temporarily selected as skeleton G_1,(Fig. 7(a)).

A series of dense points and their *LIC* value are obtained based on each skeleton curve in this skeleton, then the distribution of the largest tool radius along each skeleton curve can be determined. When two tools, T_1 and T_2, are given to mill this pocket, the feasible range of T_1 includes $G_{1,2}[b, c]$ and $G_{1,1}[d, e]$, and the feasible range of T_2 includes $G_{1,2}[a, b]$, $G_{1,2}[b, c]$, $G_{1,1}[a, d]$, $G_{1,1}[d, e]$and $G_{1,1}[e, f]$.(Fig.7(b))

2) FINAL TOOL REGION

Although one feasible tool region is machined by only one tool in actual processing, there are two or more available tools that can be found in the given toolset.

For example, as shown in Fig. 7(b), The range of the sub-skeleton curve $G_{1,2}[b, c]$ can be machined by T_1 or T_2. Therefore, to obtain a shorter processing time, the processing

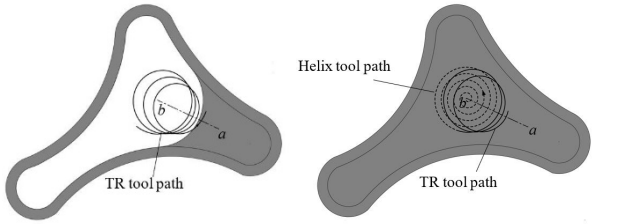

(a) One endpoint has been processed (b) One endpoint has not been processed

FIGURE 8. Selection principle of the first trochoidal centre, when machining the area represented by sub-skeleton curve $G_{1,2}[b, c]$.

time of all available tools should be calculated, then the tool with the shortest processing time is selected as the actual tool to process this feasible tool region.

Assume that two adjacent sub-skeleton curves on the one skeleton curve are processed by the same tool. The two sub-skeleton curves should be connected into a new sub-skeleton curve, and then this new sub-skeleton curve is processed with the one tool, so as to reduce the number of tool lifting.

3) SELECTION PRINCIPLE OF THE FIRST TROCHOIDAL CENTRE

When machining the area represented by the sub-skeleton curve, the first trochoidal centre must be an endpoint of this sub-skeleton curve. If the trochoidal radius of the first point on the trochoidal tool path is greater than the tool radius ($LIC \geq R_T$), the helix tool path needs to be added before the trochoidal tool path to remove the material in the circle. However, if the material in this circle has been cut by the previous tool, adding a helix tool path will lead to more idle cutting and reduce the machining efficiency (see Fig. 8). Therefore, reasonably selecting the endpoint of the sub-skeleton curve as a first trochoidal centre can shorten the trochoidal tool path and improve efficiency. The selection principle of the first trochoidal centre is as follows:

Step 1: If the material in the circle, which center is the endpoint of the sub-skeleton curve and radius equals to the *LIC* value of this endpoint, has been cut by the previous tool. Then this endpoint should be set as the first trochoidal centre. Otherwise, go to Step 2.

Step 2: If the *LIC* value of both endpoints on the sub-skeleton curve are not equal, the first trochoidal centre should be the endpoint with the larger *LIC*. Otherwise, the first trochoidal centre is random endpoints on this sub-skeleton curve.

D. SOLVING THE OPTIMIZATION MODEL BY GENETIC ALGORITHM

Since GA is generally used to solve parameter optimization problems, this paper will solve the tool optimization problem by GA to determine the optimal tool. GA mainly includes population initialization and generation evolution.

TABLE 2. Binary coding of the tool set.

Tool	Binary code
Null	0000
Ø40	0001
Ø32	0010
Ø30	0011
Ø28	0100
Ø25	0101
Ø22	0110
Ø20	0111
Ø16	1000
Ø14	1001
Ø12	1010
Ø10	1011

TABLE 3. Binary coding of the skeleton set.

Skeleton	Binary code
G_1	0000
G_2	1000
G_3	1001

1) POPULATION INITIALIZATION

Since the toolset and skeleton are parameters of the tool optimization model, the population initialization includes toolset and skeleton.

The tool in toolset Ω_o is numbered from 1 to n in ascending order of tool diameter, $\Omega_o = \{D_i \mid i = 1, 2, \cdots, n\}$, and then the coding of the cutter is that directly converting i to 0/1 binary. Of course, there also is Null-tool, which is encoded 0000. For the skeleton set of the pocket $G = \{G_k \mid k = 1, 2, \cdots, g\}$, the coding of the skeleton is to convert $k - 1$ to 0/1 binary.

For example, if given a toolset $\Omega_o = \{Ø40, Ø32, Ø30, Ø28, Ø25, Ø22, Ø20, Ø16, Ø14, Ø12, Ø10\}$, and a skeleton set $G = \{G_1, G_2, G_3\}$, the binary codes of toolset Ω_o and skeleton set G are listed in Table 2 and table 3, respectively.

After coding the individual parameters, these coded individuals should be grouped into the population, then initialize individual parameters of each population randomly.

2) GENERATION EVOLUTION

According to the principle of survival of the fittest, the optimal solution of tool optimization problem can be generated through generation evolution. The fitness value is acquired through fitness evaluation function, and then new population is generated through genetic manipulation.

Since the objective is to find the minimum total machining time of the trochoidal milling, the fitness function can be expressed as:

$$\lambda_i = \frac{1}{T_i} \tag{12}$$

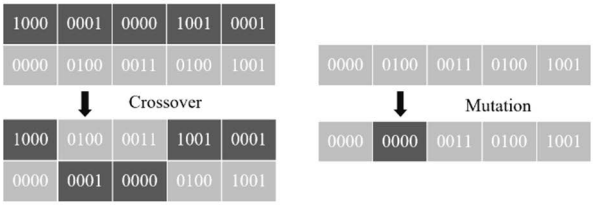

FIGURE 9. Crossover, and mutation in genetic manipulation.

where λ_i and T_i are the fitness value and machining time of the i^{th} individual, respectively. The number of individuals in the population is H.

Genetic manipulation includes selection, crossover, and mutation. The selection refers to selecting excellent individuals from the population as fathers for variation and crossover according to the selection rate. The Roulette is taken as an individual selection method in this paper. The selection rate P_i of each individual is expressed as:

$$P_i = \frac{\lambda_i}{\sum_{i=1}^{H} \lambda_i} \tag{13}$$

The selection cannot create any new individuals in the population, but it can increase the probability of individuals with high fitness in the population, and remove individuals with low fitness in the population. As shown in Fig. 9. the crossover refers to randomly selecting two individuals from the population, exchanging and combining the chromosomes of the two individuals to create two new individuals. The mutation refers to randomly selecting an individual from a population, and mutating the individual to create a new individual. After crossover (or mutation), it is necessary to check whether the new individual satisfies the requirement of available tools and rest uncut material (i.e. Satisfy the Eq. (7) and Eq. (9)). If it is, crossover (or mutation) is completed; Otherwise, repeat the crossover (or mutation) operation until it satisfies.

After calculation of all generations, the optimal tool combination and skeleton can be determined by decoding the optimal individual in the last generation population.

The maximum number of generation and population size H depend on the problem scale, such as the complexity of the processing area, the number of given tools and the maximum number of selected tools. The crossover rate is set to 0.7 and the variation rate is set to 0.01 according to experience.

IV. RESULTS AND DISCUSSION

Table 4 lists the information of the given toolset Ω_o in milling, including the diameter tool, the corresponding feed speed of the machine tool, and the corresponding step distance of the trochoidal path. A set of tools Ω will be selected from the toolset Ω_o for milling the pocket.

In order to verify the effectiveness of the method proposed in this paper, the tool selection method proposed by Ferreira et al. is used as the comparison method (Ferreira's method is shown in reference [5]).

TABLE 4. The information of the given tool set (Ω_o).

Tool serial number	Tool diameter (mm)	Step distance (mm)	Feed speed of machine tool (mm/min)
1	40	9	716
2	32	7.2	716
3	30	6.75	764
4	28	6.3	614
5	25	5.625	688
6	22	4.95	781
7	20	4.5	859
8	16	3.6	716
9	14	3.15	273
10	12	2.7	318
11	10	2.25	267

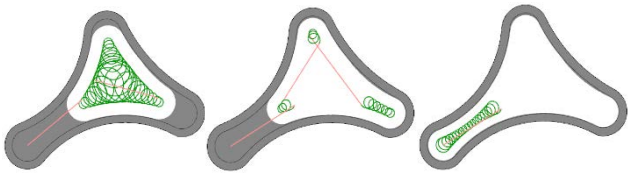

(a) Tool Ø16 (b) Tool Ø14 (c) Tool Ø10

FIGURE 10. The tool path of the Part I using the proposed method.

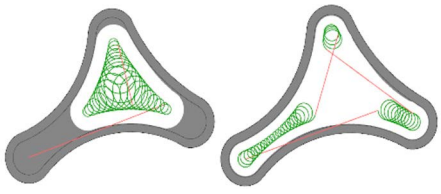

(a) Tool Ø16 (b) Tool Ø10

FIGURE 11. The tool path of the Part I using the Ferreira's method.

The proposed method has been realized by Matlab programming language. The number of skeleton curves and the computing time depends on the complexity of the processing area. Using a computer with a 6-core 2.6GHz processor, the central processing unit (CPU) time for calculating the skeleton set of the Part I shown in Fig. 2(a) was 2.5 min to 3 min.

Three tools will be selected form the toolset (Ω_o) to process the Part I and the uncut area ratio should be less than 5% ($\varepsilon = 5\%$) after processing. By applying proposed approach (The number of generations is set to 30, and the population size is set to 10.), the results of the optimal tools are Ø16, Ø14 and Ø10, and the corresponding optimal skeleton is G_2 listed in Table 1. The CPU time for solving the tool optimization model with GA is 40 min to 50 min. However, the optimal tools by applying Ferreira's method are Ø16 and Ø10.

The processing time and uncut area ratio by using these two methods is listed in Table 5. It can be seen from Table 5 that the total processing time by using the proposed method is 289 s, but that by using Ferreira's method is 327 s, which means that the efficiency of the proposed method is 11.6% higher than that of Ferreira's method. The tool path using

(a) Proposed method (b) Ferreira's method

FIGURE 12. The actual processing process of the Part I using two methods.

TABLE 5. The processing time and uncut area ratio of the part I using two methods.

	Proposed method			Ferreira's method	
Tool diameter (mm)	16	14	10	16	10
Processing time(s)	120	71	98	122	205
Cut area ratio (%)	*68.26*	10.71	16.53	*68.26*	*27.43*
Total time (s)	289			327	
Uncut area ratio (%)	4.50			4.31	

the proposed method and Ferreira's method are shown in Fig. 10 and Fig. 11, respectively.

Furthermore, comparing the tool Ø16 using these two methods, the processing area is identical, but the processing time is different. The processing time of tool Ø16 using proposed method is 120 s, but that using Ferreira's method is 122 s. Obviously, the processing efficiency of tool Ø16 using the proposed approach is increased by 1.6% compared to using the Ferreira's method. The main reason for this case is that the skeletons of the two methods are different. Therefore, the skeleton has influence on the tool path and processing time of trochoidal milling.

The actual processing process using the two methods is shown in Fig. 12.

Fig. 13(a) shows an example of a pocket for 2.5D milling. The skeleton set of this pocket is obtained by using the method presented in Section 2. The number of elements in this skeleton set is 4096, and the CPU time for calculating this skeleton set was 8 h to 9 h.

Suppose the three cutting tools in set (Ω_o) are selected and the minimum the uncut area ratio of the Part II after processing is 2%, the optimal tools (Ø32, Ø22, and Ø16) and skeleton (See Fig. 13(b)) can be determined by using the proposed approach. The CPU time for solving the tool optimization model with GA is 16 h to 17 h, in case of the number of generations and the population size is set to 100 and 10, respectively.

Furthermore, the region division represented by sub-skeleton curves is shown in Fig. 13(c), and the corresponding tool path is shown in Fig.14. However, the optimal tools by using the Ferreira's method are Ø32, Ø20 and Ø10, whereas the corresponding tool path is shown in Fig. 15.

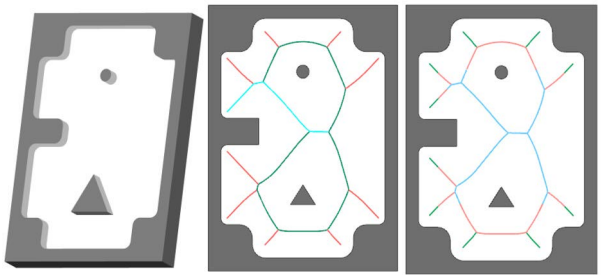

(a) Part II (b) Optimal skeleton (c) Region division

FIGURE 13. Part II model, the skeleton, and the region division represented by sub-skeleton curves.

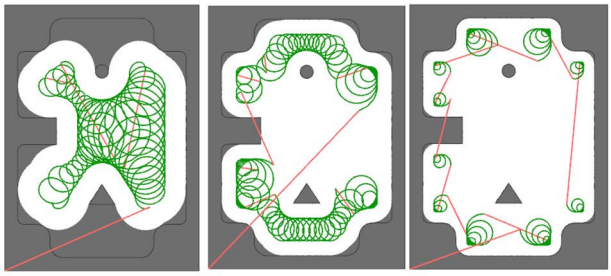

(a) Tool Ø32 (b) Tool Ø22 (c) Tool Ø16

FIGURE 14. The tool path of the Part II using the proposed method.

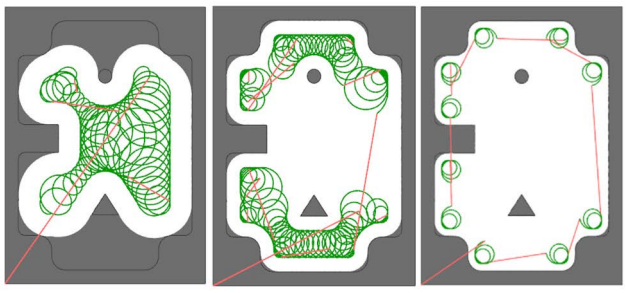

(a) Tool Ø32 (b) Tool Ø20 (c) Tool Ø10

FIGURE 15. The tool path of the Part II using the Ferreira's method.

The processing time and uncut area ratio by using two method is listed in Table 6. It is apparent that the total processing time by using the proposed approach is 695 s, while that by using the Ferreira's method is 893 s. The processing efficiency of the proposed approach is increased by 22.2% compared to the Ferreira's method. It is verified again that the proposed approach can improve the processing efficiency of trochoidal milling.

In addition, although the cut area ratio of tool Ø32 using these two methods is 74.30%, the processing efficiency of the tool Ø32 using the proposed approach is increased by 4.4% compared to using the Ferreira's method.

It is proved again that the skeleton has an impact on the processing time and tool path of trochoidal milling. The influence of the skeleton on trochoidal milling increases with

(a) Proposed method (b) Ferreira's method

FIGURE 16. The actual processing process of the part II using two methods.

TABLE 6. The processing time and uncut area ratio of the part II using two methods.

	Proposed method			Ferreira's method		
Tool diameter (mm)	32	22	16	32	20	10
Processing time(s)	329	249	117	344	298	251
Cut area ratio (%)	74.30	21.50	2.55	74.30	22.92	1.15
Total time (s)	695			893		
Uncut area ratio (%)	1.65			1.63		

the complexity of the skeleton. The actual processing process using the two methods is shown in Fig. 16.

Although the calculation amount and computer running time of the proposed method is large, the proposed method can significantly improve the machining efficiency. This method is applied to other pockets for selecting cutting tools in trochoidal milling, the optimal tool combination and corresponding skeleton can be obtained correctly. It shows that the stability and robustness of this algorithm is strong to a certain extent.

V. CONCLUSION

A multi-tool selection method for 2 1/2-axis trochoidal milling of the pocket based on optimal skeleton is proposed in this paper. The main contributions can be summarized as follows:

1) Through the establishment of skeleton extraction method, the skeleton of the pocket can be obtained after the preliminary skeleton set was extracted according to the principle of medial axis transformation, and then the skeleton set can be acquired by repeatedly extracting the skeleton. The successful extraction of the skeleton set provides a basis for scientific selection of trochoidal cutter.
2) Aiming at the shortest machining time, a tool selection model based on skeleton optimization is established in this paper. After solving the optimization model by GA, the optimal tool combination and skeleton can be obtained simultaneously.
3) The experimental results show that the processing efficiency of the selected tool using the method proposed in this paper is higher than that of the Ferreira's method, and the more complex of the pocket, the higher the efficiency and the more obvious the advantage of the tool optimization algorithm proposed in this paper.

REFERENCES

[1] M. Luo, C. Hah, and H. M. Hafeez, "Four-axis trochoidal toolpath planning for rough milling of aero-engine blisks," *Chin. J. Aeronaut.*, vol. 32, no. 8, pp. 2009–2016, Aug. 2019, doi: 10.1016/j.cja.2018.09.001.

[2] G. U. Pelayo, D. Olvera-Trejo, M. Luo, K. Tang, L. N. L. D. Lacalle, and A. Elías-Zuñiga, "A model-based sustainable productivity concept for the best decision-making in rough milling operations," *Measurement*, vol. 186, Dec. 2021, Art. no. 110120, doi: 10.1016/j.measurement.2021.110120.

[3] A. Maldonado-Macías, A. Alvarado, J. L. García, and C. O. Balderrama, "Intuitionistic fuzzy TOPSIS for ergonomic compatibility evaluation of advanced manufacturing technology," *Int. J. Adv. Manuf. Technol.*, vol. 70, nos. 9–12, pp. 2283–2292, Feb. 2014, doi: 10.1007/s00170-013-5444-5.

[4] Z.-H. Xiong, C.-G. Zhuang, and H. Ding, "Curvilinear tool path generation for pocket machining," *Proc. Inst. Mech. Eng., B, J. Eng. Manuf.*, vol. 225, no. 4, pp. 483–495, Apr. 2011, doi: 10.1177/2041297510394085.

[5] J. C. Ferreira and D. M. Ochoa, "A method for generating trochoidal tool paths for 21/2D pocket milling process planning with multiple tools," *Proc. Inst. Mech. Eng., B, J. Eng. Manuf.*, vol. 227, no. 9, pp. 1287–1298, Sep. 2013, doi: 10.1177/0954405413487897.

[6] D. M. O. Gonzáles, "Método de geração de trajetórias trocoidais e espirais combinadas para o fresamento de desbaste de cavidades 2, 5D com múltiplas ferramentas," Universidade Federal de Santa Catarina, Brazil, 2013. [Online]. Available: https://repositorio.ufsc.br/xmlui/handle/123456789/106820

[7] S. Hinduja and D. Sandiford, "An optimum two-tool solution for milling $2^{1/2}$D features from technological and geometric viewpoints," *CIRP Ann.*, vol. 53, no. 9, pp. 77–80, 2004, doi: 10.1016/S0007-8506(07)60649-0.

[8] W. Shixiong, M. Wei, L. Bin, and W. Chengyong, "Trochoidal machining for the high-speed milling of pockets," *J. Mater. Process. Technol.*, vol. 233, pp. 29–43, Jul. 2016, doi: 10.1016/j.jmatprotec.2016.01.033.

[9] H. Ramaswami, R. S. Shaw, and S. Anand, "Selection of optimal set of cutting tools for machining of polygonal pockets with islands," *Int. J. Adv. Manuf. Technol.*, vol. 53, nos. 9–12, pp. 963–977, Apr. 2011, doi: 10.1007/s00170-010-2909-7.

[10] D. Veeramani and Y. S. Gau, "Selection of an optimal set of cutting-tool sizes for 212D pocket machining," *Comput.-Aided Des.*, vol. 29, no. 12, pp. 869–877, 1997, doi: 10.1016/S0010-4485(97)00042-0.

[11] X. L. Phung, H. S. Truong, and N. T. Bui, "Expert system based on integrated fuzzy AHP for automatic cutting tool selection," *Appl. Sci.*, vol. 9, no. 20, p. 4308, Oct. 2019, doi: 10.3390/app9204308.

[12] W. Ba, N. Ren, and L. Cao, "Geometry of 3D MAT and its application to moulding surfaces," *Graph. Models*, vol. 82, pp. 1–12, Nov. 2015, doi: 10.1016/j.gmod.2015.09.004.

[13] X. Li, J. Ren, X. Lv, and K. Tang, "Collaborative optimization of conical cutter sequence for efficient multi-axis machining of deep curved cavities," *J. Manuf. Processes*, vol. 66, pp. 407–423, Jun. 2021, doi: 10.1016/j.jmapro.2021.03.049.

[14] K. N. Shi, N. Liu, S. B. Wang, J. X. Ren, and Y. Yuan, "Experimental and theoretical investigation of milling tool selection towards energy-efficient process planning in discrete parts manufacturing," *Int. J. Adv. Manuf. Technol.*, vol. 104, nos. 1–4, pp. 1099–1107, Sep. 2019, doi: 10.1007/s00170-019-03960-3.

[15] C. B. Li, W. Lei, H. Shen, and T. Wan, "Optimization of tool combination selection in 2.5D pocket NC milling for energy consumption reduction," *Comput. Integr. Manuf. Syst.*, vol. 23, no. 2, pp. 293–304, 2017, doi: 10.13196/j.cims.2017.02.008.

[16] G. Zhao, K. Cheng, W. Wang, Y. Liu, and Z. Dan, "A milling cutting tool selection method for machining features considering energy consumption in the STEP-NC framework," *Int. J. Adv. Manuf. Technol.*, vol. 120, nos. 5–6, pp. 3963–3981, May 2022, doi: 10.1007/s00170-022-08964-0.

[17] J. Wang, M. Luo, H. M. Hafeez, and D. Zhang, "Image skeleton and GA based tool selection for 2 1/2-axis rough milling," *IEEE Access*, vol. 6, pp. 32566–32575, 2018, doi: 10.1109/ACCESS.2018.2842091.
[18] B. K. Jayanthi, "Multiple cutting tool selection in automated process planning & CNC code generation," Penn State Univ. Libraries, USA, 2014. [Online]. Available: https://etda.libraries.psu.edu/catalog/23670
[19] Y. Zhou, G. Zhi, W. Chen, Q. Qian, D. He, B. Sun, and W. Sun, "A new tool wear condition monitoring method based on deep learning under small samples," *Measurement*, vol. 189, Feb. 2022, Art. no. 110622, doi: 10.1016/j.measurement.2021.110622.
[20] Y. Zhou, B. Sun, and W. Sun, "A tool condition monitoring method based on two-layer angle kernel extreme learning machine and binary differential evolution for milling," *Measurement*, vol. 166, Dec. 2020, Art. no. 108186, doi: 10.1016/j.measurement.2020.108186.
[21] D. Checa, G. Urbikain, A. Beranoagirre, A. Bustillo, and L. N. L. D. Lacalle, "Using machine-learning techniques and virtual reality to design cutting tools for energy optimization in milling operations," *Int. J. Comput. Integr. Manuf.*, vol. 35, no. 9, pp. 951–971, Sep. 2022, doi: 10.1080/0951192X.2022.2027020.
[22] W. Che, X. Yang, and G. Wang, "Skeleton-driven 2D distance field metamorphosis using intrinsic shape parameters," *Graph. Models*, vol. 66, no. 2, pp. 102–126, Mar. 2004, doi: 10.1016/j.gmod.2003.11.001.
[23] B. R. C. Karuppanan and M. Saravanan, "Optimized sequencing of CNC milling toolpath segments using Metaheuristic algorithms," *J. Mech. Sci. Technol.*, vol. 33, no. 2, pp. 791–800, Feb. 2019, doi: 10.1007/s12206-019-0134-3.
[24] G. Elber, E. Cohen, and S. Drake, "MATHSM: Medial axis transform toward high speed machining of pockets," *Comput.-Aided Des.*, vol. 37, no. 2, pp. 241–250, Feb. 2005, doi: 10.1016/j.cad.2004.05.008.
[25] M. Otkur and I. Lazoglu, "Trochoidal milling," *Int. J. Mach. Tools Manuf.*, vol. 47, no. 9, pp. 1324–1332, Jul. 2007, doi: 10.1016/j.ijmachtools.2006.08.002.
[26] Q.-H. Wang, S. Wang, F. Jiang, and J.-R. Li, "Adaptive trochoidal toolpath for complex pockets machining," *Int. J. Prod. Res.*, vol. 54, no. 20, pp. 5976–5989, Oct. 2016, doi: 10.1080/00207543.2016.1143135.
[27] X. Huang, S. Wu, L. Liang, X. Li, and N. Huang, "Efficient trochoidal milling based on medial axis transformation and inscribed ellipse," *Int. J. Adv. Manuf. Technol.*, vol. 111, nos. 3–4, pp. 1069–1076, Nov. 2020, doi: 10.1007/s00170-020-06172-2.
[28] J. Wang, M. Luo, B. H, Wu, and D. H. Zhang, "A trochoidal path planning method for rough machining of aeroengine casing parts," *Acta Aeronautica et Astronautica Sinica*, vol. 39, no. 6, pp. 216–227, 2018, doi: 10.7527/S1000-6893.2017.21814.

FEIYAN HAN was born in Xianyang, China, in 1983. She received the B.S. degree in mechanical manufacturing and automation from the Xi'an University of Technology, in 2006, and the M.S. and Ph.D. degrees in aerospace manufacturing engineering from Northwestern Polytechnical University, in 2012 and 2016, respectively. She is currently a Postdoctoral Fellow with the School of Mechanical Engineering, Xi'an University of Science and Technology, China. Her research interests include computer aided geometric design of complex surfaces and multi-axis CNC milling.

LONGLONG HE was born in Xi'an, China, in 1998. She received the B.S. degree in mechanical manufacturing and automation from the Xi'an University of Science and Technology, in 2020, where she is currently pursuing the master's degree in machinery manufacturing. Her research interests include CNC milling and automatic processing.

ZHITAO HU was born in Jiujiang, China, in 1996. He received the B.S. degree in mechanical manufacturing and automation from the Nanyang Institute of Technology, in 2020. He is currently pursuing the master's degree in machinery manufacturing with the Xi'an University of Science and Technology. His research interests include reuse of complex surface machining knowledge and CNC machining.

CHUANWEI ZHANG received the B.S. and M.S. degrees in mechanical engineering from the Xi'an University of Science and Technology, in 1998 and 2001, respectively, and the Ph.D. degree in mechanical engineering from Xi'an Jiaotong University, China, in 2006. He is currently a Professor at the Xi'an University of Science and Technology. His research interests include intelligent manufacturing, intelligent connected vehicle, and mining vehicles.